Inorganic Chemistry

Article

pubs.acs.org/IC

Improving the Efficiency of the Photoinduced Charge-Separation Process in a Rhenium(I)−Zinc Porphyrin Dyad by Simple Chemical Functionalization

Teresa Gatti,[†,‡] Paolo Cavigli,[†] Ennio Zangrando,[†] Elisabetta Iengo,*[,†] Claudio Chiorboli,[§] and Maria Teresa Indelli*[,⊥]

[†]Department of Chemical and Pharmaceutical Sciences, University of Trieste, Via L. Giorgieri 1, 34127 Trieste, Italy

[§]ISOF-CNR Sezione di Ferrara, Via L. Borsari 40, 44100 Ferrara, Italy

[⊥]Department of Chemistry, University of Ferrara, Via L. Borsari 46, 44100 Ferrara, Italy

Supporting Information

ABSTRACT: We demonstrate here that, whereas the rhenium(I)−zinc porphyrin dyad *fac*-[Re(CO)$_3$(bpy)(Zn·4′MPyP)](CF$_3$SO$_3$) [**1**; 4′MPyP = 5-(4′-pyridyl)-10,15,20-triphenylporphyrin] shows no evidence for photoinduced electron transfer upon excitation in the visible region because the charge-separated state ZnP$^+$−Re$^-$ is almost isoenergetic with the singlet excited state of the zinc porphyrin (ΔG = −0.05 eV), the introduction of electron-withdrawing ethyl ester groups on the bpy ligand significantly improves the thermodynamics of the process (ΔG = −0.42 eV). As a consequence, in the new dyad *fac*-[Re(CO)$_3$(4,4′-DEC-bpy)(Zn·4′MPyP)](CF$_3$SO$_3$) (**4**; 4,4′-DEC-bpy = 4,4′-diethoxycarbonyl-2,2′-bipyridine), an efficient and ultrafast intramolecular electron-transfer process occurs from the excited zinc porphyrin to the rhenium unit upon excitation with visible light. Conversely, the introduction of electron-donor *tert*-butyl groups on the *meso*-phenyl moieties of the zinc porphyrin has a negligible effect on the photophysics of the system. For dyad **4**, the time constants for the charge-separation and charge-recombination processes in solvents of different polarity (PrCN, DCM, and toluene) were measured by an ultrafast time-resolved absorption technique (λ_{exc} = 560 nm).

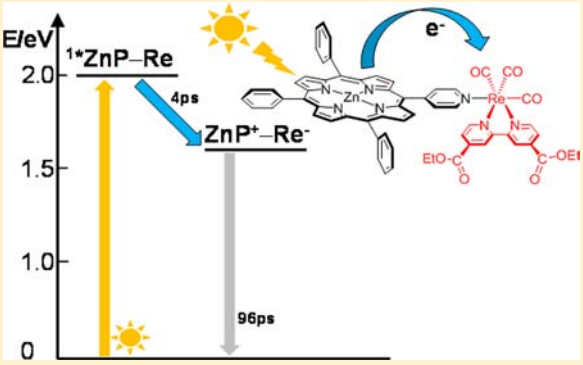

INTRODUCTION

In the field of photocatalysis, the preparation of simple, easy-to-make, and robust dyads and triads is a topic of great research interest. Such systems, in fact, might afford efficient exploitation of solar light for performing tantalizing, but so far elusive, reactions, such as CO_2 or water reduction.[1] The minimal system to be used for a photoinduced reduction process is a dyad formed by a chromophore unit, which must also be a good electron donor in its excited state (D), connected to a good electron-acceptor unit (A). In other words, the photoactive unit must absorb light, preferentially in the visible region, and then rapidly transfer an electron from its excited state to the other fragment; the latter thus becomes a powerful reducing agent capable of performing a rapid reduction of the substrate (Figure 1). For an efficient process, the rate of the reduction must be faster than the recombination step. In particular, dyads in which a rhenium(I) tricarbonyldiimine complex is bound to a photosensitizer, of either organic or inorganic nature, that absorbs in the visible range are actively investigated as catalysts for the photoreduction of CO_2 to CO.[2]

In this context, in recent years we described simple rhenium(I) porphyrin conjugates, in which a zinc pyridylporphyrin chromophore, which behaves as both photoactive and

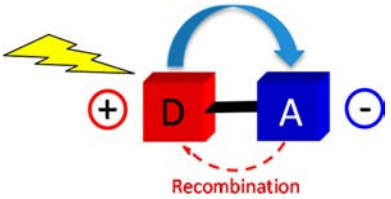

Figure 1. Schematic representation of the photoinduced electron-transfer process in a generic dyad.

electron-donor moieties, is directly coordinated to one or more peripheral electron-acceptor *fac*-[Re(CO)$_3$(bpy)]$^+$ fragments.[3] One example is *fac*-[Re(CO)$_3$(bpy)(Zn·4′MPyP)](CF$_3$SO$_3$) [**1**; 4′MPyP = 5-(4′-pyridyl)-10,15,20-triphenylporphyrin and bpy = bipyridine]. These compounds proved to be very stable in solution, also upon excitation, and were structurally characterized in solution and in the solid state. However, a detailed photophysical study showed no evidence for photoinduced electron transfer in dyad **1** because the charge-separated state ZnP$^+$−Re$^-$ is almost isoenergetic with the

Received: December 5, 2012
Published: March 5, 2013

   dx.doi.org/10.1021/ic302663c | *Inorg. Chem.* 2013, 52, 3190−3197

Scheme 1. Photoinduced Electron-Transfer Process in the Rhenium(I)−Zinc Porphyrin Dyad 1

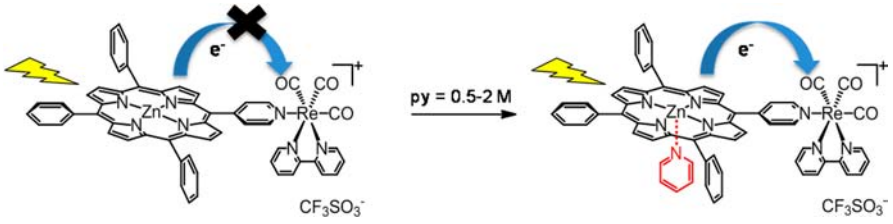

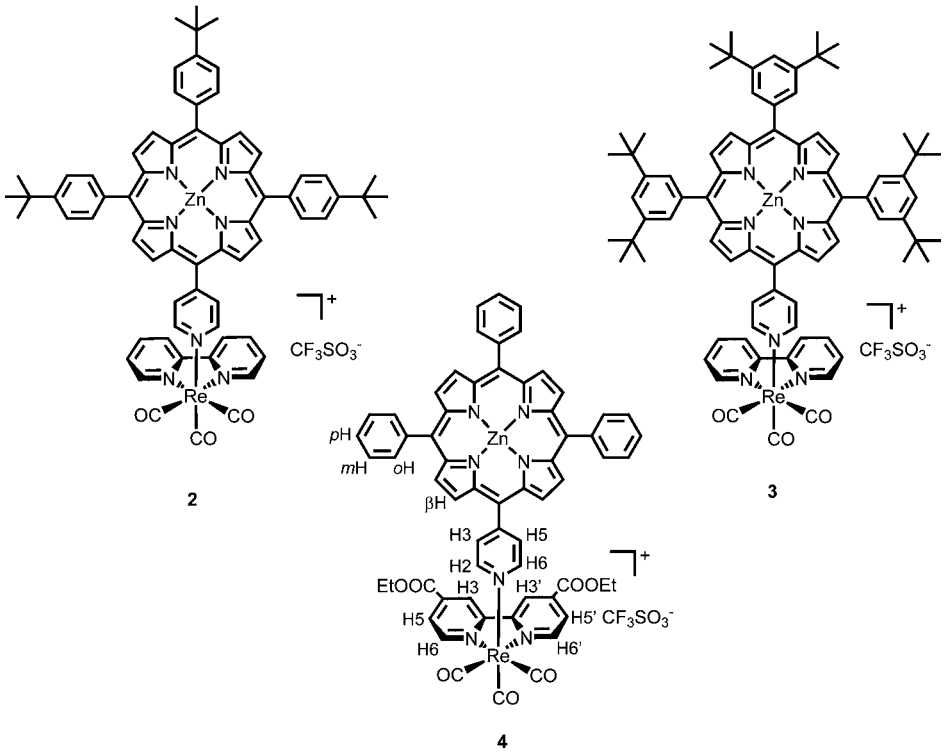

Figure 2. Functionalized rhenium(I)−zinc porphyrin dyads **2**−**4** with a numbering scheme for the NMR spectra.

singlet excited state of the zinc porphyrin unit. Nevertheless, in the presence of pyridine (which binds axially to zinc and thus affects the porphyrin oxidation potential), a moderately efficient photoinduced electron-transfer process from the zinc porphyrin to the Re(bpy) unit was observed upon excitation in the visible region (Scheme 1). This result led us to predict that an appropriate functionalization of the bpy ligand and/or of the porphyrin chromophore, with a judicious choice of electron-donor and electron-withdrawing substituents, might improve the thermodynamics, and thus the efficiency, of the photoinduced electron-transfer process.[3]

Here we report on the results obtained following this approach and demonstrate that, whereas the introduction of electron-donor *tert*-butyl (*t*Bu) groups (either three or six) on the *meso*-phenyl moieties of the zinc porphyrin has a negligible effect on the photophysics of the system [dyads *fac*-[Re(CO)$_3$(bpy)(Zn·4′MPy*t*BuP)](CF$_3$SO$_3$) (**2**) and *fac*-[Re(CO)$_3$(bpy)(Zn·4′MPyd*t*BuP)](CF$_3$SO$_3$) (**3**); Figure 2], the introduction of electron-withdrawing ethyl ester groups on the bpy ligand led to the expected results, and the dyad *fac*-[Re(CO)$_3$(4,4′-DEC-bpy)(Zn·4′MPyP)](CF$_3$SO$_3$) (**4**; 4,4′-DEC-bpy = 4,4′-diethoxycarbonyl-2,2′-bipyridine; Figure 2) efficiently yields the charge-separated state ZnP$^+$−Re$^-$ upon excitation with visible light.

EXPERIMENTAL SECTION

Instrumental Methods. Mono- and bidimensional (H−H COSY) ^{1}H NMR spectra were recorded on a JEOL Eclipse 400FT (400 MHz) or a Varian 500 (500 MHz) spectrometer. All spectra were run at room temperature; ^{1}H chemical shifts were referenced to the peak of residual nondeuterated solvent (δ = 7.26 ppm for CDCl$_3$, 2.04 ppm for acetone-d_6, 3.30 ppm for CD$_3$OD, and 4.33 ppm for CD$_3$NO$_2$). Electrospray ionization mass spectrometry (ESI-MS) measurements were performed on a Perkin-Elmer APII spectrometer at 5600 eV by Dr. Fabio Hollan, Department of Chemical and Pharmaceutical Sciences, University of Trieste, Italy. Solution (CHCl$_3$) IR spectra were recorded in 0.1 mm cells with NaCl windows on a Perkin-Elmer Fourier transform infrared/Raman 2000 instrument in the transmission mode. UV/vis absorption spectra were recorded with a Jasco V-570 UV/vis/near-IR spectrophotometer. Emission spectra were acquired on a Spex-Jobin Ivon Fluoromax-2 spectrofluorimeter, equipped with Hamamatsu R3896 tubes. Nanosecond emission lifetimes were measured using a TCSPC apparatus (PicoQuant Picoharp300) equipped with subnanosecond LED sources (280−600 nm range; 500−700 ps pulse width) powered with a PicoQuant PDL 800-B variable-pulsed (2.5−40 MHz) power supply. The decays were analyzed by means of PicoQuant FluoFit Global Fluorescence Decay Analysis Software. Femtosecond time-resolved experiments were performed using a pump−probe setup based on a Spectra-Physics Hurricane Ti:sapphire laser source and an Ultrafast Systems Helios spectrometer.[4] The 560 nm pump pulses were generated with a Spectra Physics 800 optical parametric amplifier. Probe pulses were

dx.doi.org/10.1021/ic302663c | *Inorg. Chem.* 2013, 52, 3190−3197

obtained by continuum generation on a sapphire plate (useful spectral range: 450−800 nm). The effective time resolution was ca. 300 fs, the temporal chirp over the white-light 450−750 nm range was ca. 200 fs, and the temporal window of the optical delay stage was 0−1000 ps. The time-resolved spectral data were analyzed with Ultrafast Systems Surface Explorer Pro software.

Crystallographic data for compound **2** were collected at the X-ray diffraction beamline of the synchrotron Elettra (Trieste) at 100 K, λ = 1.0000 Å; those for *fac*-[Re(CO)$_3$(4,4′-DEC-bpy)(py)](CF$_3$SO$_3$) (**7**) were collected on a Nonius DIP-1030H single-crystal diffractometer (Mo Kα radiation, λ = 0.71073 Å) at room temperature. Cell refinement, indexing, and scaling of the data sets were performed using programs *Denzo* and *Scalepack*.[5] Both structures were solved by direct methods and subsequent Fourier analyses[6] and refined by the full-matrix least-squares method based on F^2 with all observed reflections.[6] The triflate anion in **2** was found to be disordered over two positions, each refined with an occupancy of 0.50. Hydrogen atoms were placed at calculated positions. All of the calculations were made using *WinGX*, version 1.80.05.[7]

Materials. Tetraphenylporphyrin (TPP) and the corresponding *t*Bu-substituted TPPs 5,10,15,20-tetrakis(4′-*tert*-butylphenyl)-porphyrin (*t*BuTPP) and 5,10,15,20-tetrakis(3′,5′-*tert*-butylphenyl)-porphyrin (d*t*BuTPP) and 5-(4′-pyridyl)-10,15,20-triphenylporphyrin (4′MPyP) and the corresponding *t*Bu-substituted MPyPs 5-(4′-pyridyl)-10,15,20-tris(4′-*tert*-butylphenyl)porphyrin (4′MPy*t*BuP) and 5-(4′-pyridyl)-10,15,20-tris(3′,5′-*tert*-butylphenyl)porphyrin (4′MPyd*t*BuP) were synthesized and purified as described in the literature.[8] The substituted ligand 4,4′-diethoxycarbonyl-2,2′-bipyridine (4,4′-DEC-bpy) was also prepared as described in the literature.[9]

Synthesis of the Rhenium(I) Complexes and Rhenium(I) Porphyrin Conjugates. Preparation of the *fac*-[Re(CO)$_3$(4,4′-DEC-bpy)(DMSO-O)](CF$_3$SO$_3$) (**6**) precursor was similar to that previously described by us for *fac*-[Re(CO)$_3$(bpy)(DMSO-O)]-(CF$_3$SO$_3$) (**5**).[10] The dyads **2** and **3** were prepared using procedures similar to that described by us for **1**.[3] The dyad **4** and model compounds **7** and *fac*-[Re(CO)$_3$(bpy)(py)](CF$_3$SO$_3$) were similarly prepared from complexes **6** and **5**, respectively.

***fac*-[Re(CO)$_3$(4,4′-DEC-bpy)(DMSO-O)](CF$_3$SO$_3$) (6).** *fac*-[Re-(CO)$_3$(DMSO-O)$_3$](CF$_3$SO$_3$) (100 mg, 0.15 mmol) and 4,4′-DEC-bpy (50 mg, 0.17 mmol) were dissolved in acetone (15 mL). The solution, initially colorless, was refluxed for 1 h under an argon atmosphere and turned yellow. Concentration to ca. 7 mL followed by the addition of *n*-hexane (3 mL) induced in a few days the formation of microcrystals, which were removed by filtration, washed with *n*-hexane, and vacuum-dried. Yield: 77 mg (65%). ^{1}H NMR (δ, 400 MHz, CD$_3$NO$_2$): 9.32 (d, J = 5.7 Hz, 2H, H6,6′), 9.08 (s, 2H, H3,3′), 8.25 (d, J = 5.6 Hz, 2H, H5,5′), 4.52 (q, J = 7.1 Hz, 4H, CH$_2$), 2.60 (s, 6H, DMSO-O), 1.45 (t, J = 7.1 Hz, 6H, CH$_3$).

***fac*-[Re(CO)$_3$(4,4′-DEC-bpy)(py)](CF$_3$SO$_3$) (7).** To a solution of complex **6** (50 mg, 0.06 mmol) in CH$_2$Cl$_2$ (20 mL) was added pyridine (30 μL, 0.3 mmol). The solution was stirred for 1 day at room temperature and then concentrated in vacuo to ca. 5 mL. Yellow microcrystals of pure product formed upon the dropwise addition of *n*-hexane until saturation and were removed by filtration, washed with *n*-hexane, and vacuum-dried. Yield: 85%. Crystals of **7** suitable for X-ray diffraction were obtained by the slow diffusion of *n*-hexane into a dichloromethane (DCM) solution of the complex. ^{1}H NMR (δ, 400 MHz, CDCl$_3$): 9.27 (d, J = 5.6 Hz, 2H, H6,6′), 9.02 (s, 2H, H3,3′), 8.31 (m, 4H, H5,5′ + H2,6 py), 7.83 (t, J = 7.7 Hz, 1H, H4 py), 7.47 (t, J = 7.6 Hz, 2H, H3,5 py), 4.57 (q, J = 7.2 Hz, 4H, CH$_2$), 1.50 (t, J = 7.2 Hz, 6H, CH$_3$). IR (cm^{-1}, CHCl$_3$): 2038 (s, $\tilde{\nu}_{C=O\ fac}$), 1945 (s, br, $\tilde{\nu}_{C=O\ fac}$), 1935 (s, br, $\tilde{\nu}_{C=O\ fac}$), 1726 (m, $\tilde{\nu}_{C=O}$).

Crystal data: C$_{25}$H$_{21}$F$_3$N$_3$O$_{10}$ReS, MW = 798.71, triclinic, space group $P\bar{1}$, a = 10.710(2) Å, b = 15.457(2) Å, c = 18.150(3) Å, α = 80.300(11)°, β = 80.564(12)°, γ = 79.363(9)°, V = 2883.3(8) Å^3, Z = 4, D_c = 1.840 g/cm^3, μ(Mo Kα) = 4.366 mm^{-1}, F(000) = 1560, θ range = 1.35−29.13°. Final R1 = 0.0434, wR2 = 0.1148, and S = 0.937 for 779 parameters and 15035 unique reflections [R(int) = 0.0420], of which 9292 with $I > 2\sigma(I)$, max positive and negative peaks in ΔF map 1.048 and −0.935 e/Å^3.

***fac*-[Re(CO)$_3$(bpy)(4′MPy*t*BuP)](CF$_3$SO$_3$) (8).** 4′MPy*t*BuP (90 mg, 0.12 mmol) and **5** (60 mg, 0.09 mmol) were dissolved in CHCl$_3$ (25 mL). The mixture was heated to reflux for 8 h and then concentrated in vacuo to ca. 15 mL. The product precipitated as a purple solid upon the addition of diethyl ether until saturation and was collected by filtration, washed with diethyl ether, and vacuum-dried. Yield: 87 mg (71%). ^{1}H NMR (δ, 400 MHz, acetone-d_6): 9.70 (d, J = 5.3 Hz, 2H, H6,6′), 9.03 (d, J = 6.4 Hz, 2H, H2,6), 8.95 (d, J = 8.3 Hz, 2H, H3,3′), 8.85 (m, 8H, βH), 8.61 (t, J = 7.7 Hz, 2H, H4,4′), 8.34 (d, J = 6.5 Hz, 2H, H3,5), 8.18 (d, J = 8.1 Hz, 2H, *o*H), 8.15 (d, J = 8.0 Hz, 4H, *o*H), 8.12 (t, J = 8.0 Hz, 2H, H5,5′), 7.85 (m, 6H, *m*H), 1.60 (s, 27H, *t*Bu), −2.86 (s, 2H, NH). ESI-MS. Calcd for C$_{68}$H$_{61}$N$_7$O$_3$Re ([M − CF$_3$SO$_3$]$^+$): 1210.5. Found: 1210.4. IR (cm^{-1}, CHCl$_3$): 2038 (s, $\tilde{\nu}_{C=O\ fac}$), 1930 (s, br, $\tilde{\nu}_{C=O\ fac}$).

***fac*-[Re(CO)$_3$(bpy)(4′MPyd*t*BuP)](CF$_3$SO$_3$) (9).** 4′MPyd*t*BuP (180 mg, 0.18 mmol) and **5** (90 mg, 0.14 mmol) were dissolved in CHCl$_3$ (20 mL). The mixture was heated to reflux for 8 h and then concentrated in vacuo to ca. 8 mL. The dropwise addition of *n*-hexane (5 mL) induced precipitation of the product as a microcrystalline purple solid, which was collected by filtration and recrystallized from acetone/*n*-hexane. Yield: 150 mg (76%). ^{1}H NMR (δ, 400 MHz, CDCl$_3$): 9.26 (d, J = 4.7 Hz, 2H, H6,6′), 9.17 (d, J = 8.4 Hz, 2H, H3,3′), 8.90 (m, 6H, βH), 8.61 (d, 2 J = 4.9 Hz, H, βH), 8.53 (d, J = 6.5 Hz, 2H, H2,6), 8.48 (t, J = 7.2 Hz, 2H, H4,4′), 8.21 (d, J = 6.5 Hz, 2H, H3,5), 8.03 (d, J = 1.8 Hz, 2H, *o*H), 8.01 (d, J = 1.8 Hz, 4H, *o*H), 7.83 (t, J = 6.5 Hz 2H, H5,5′), 7.78 (m, 3H, *p*H), 1.50 (s, 54H, *t*Bu), −2.78 (s, 2H, NH). ESI-MS. Calcd for C$_{80}$H$_{85}$N$_7$O$_3$Re ([M − CF$_3$SO$_3$]$^+$): 1378.6. Found: 1378.9. IR (cm^{-1}, CHCl$_3$): 2038 (s, $\tilde{\nu}_{C=O\ fac}$), 1930 (s, br, $\tilde{\nu}_{C=O\ fac}$).

***fac*-[Re(CO)$_3$(4,4′-DEC-bpy)(4′MPyP)](CF$_3$SO$_3$) (10).** 4′MPyP (50 mg, 0.09 mmol) and **6** (60 mg, 0.08 mmol) were dissolved in CHCl$_3$ (15 mL), and the solution was heated to reflux for 8 h. After concentration to ca. 8 mL, *n*-hexane (10 mL) was added to induce precipitation of the product as a purple solid, which was collected by filtration, washed thoroughly with *n*-hexane, and vacuum-dried. Yield: 70 mg (72%). ^{1}H NMR (δ, 400 MHz, CDCl$_3$): 9.58 (d, J = 5.6 Hz, 2H, H6,6′), 9.15 (s, 2H, H3,3′), 8.83 (m, 6H, βH), 8.76 (d, J = 6.2 Hz, 2H, H2,6), 8.65 (d, J = 3.3 Hz, 2H, βH), 8.43 (d, J = 4.7 Hz, 2H, H5,5′), 8.28 (d, J = 6.1 Hz, 2H, H3,5), 8.19 (d, J = 8.0 Hz, 2H, *o*H), 8.17 (d, J = 7.5 Hz, 4H, *o*H), 7.74 (m, 9H, *m*+*p*H), 4.55 (q, J = 7.1 Hz, 4H, CH$_2$), 1.47 (t, J = 7.1 Hz, 6H, CH$_3$), −2.88 (s, 2H, NH). ESI-MS. Calcd for C$_{62}$H$_{45}$N$_7$O$_7$Re ([M − CF$_3$SO$_3$]$^+$): 1186.3. Found: 1186.5. IR (cm^{-1}, CHCl$_3$): 2037 (s, $\tilde{\nu}_{C=O\ fac}$), 1931 (s, br, $\tilde{\nu}_{C=O\ fac}$), 1733 (m, $\tilde{\nu}_{C=O}$).

Zinc Adducts. The insertion of zinc into the free-base porphyrins and rhenium(I) pyridylporphyrin conjugates was performed according to this general procedure: a concentrated CHCl$_3$ solution of each adduct was treated overnight with an 8-fold molar excess of Zn(CH$_3$COO)$_2$·2H$_2$O dissolved in a minimum amount of methanol (MeOH). The solvent was evaporated in vacuo and the solid redissolved in CHCl$_3$. The product was precipitated by the addition of *n*-hexane, removed by filtration, washed thoroughly with cold MeOH and diethyl ether, and vacuum-dried. Yield: >85%. The compounds were characterized by ^{1}H NMR and IR spectroscopy and ESI-MS.

***fac*-[Re(CO)$_3$(bpy)(Zn·4′MPy*t*BuP)](CF$_3$SO$_3$) (2).** Yield: 85%. ^{1}H NMR (δ, 400 MHz, CD$_3$OD): 9.54 (d, J = 5.6 Hz, 2H, H6,6′), 8.85 (d, J = 4.7 Hz, 2H, H3,3′), 8.82 (m, 6H, βH), 8.76 (d, J = 6.5 Hz, 2H, H2,6), 8.57 (d, J = 4.7 Hz, 2H, βH), 8.44 (t, J = 8.0 Hz, 2H, H4,4′), 8.19 (d, J = 6.5 Hz, 2H, H3,5), 8.07 (d, J = 5.9 Hz, 2H, *o*H), 8.05 (d, J = 5.9 Hz, 4H, *o*H), 7.97 (t, J = 6.7 Hz, 2H, H5,5′), 7.77 (m, 6H, *m*H), 1.60 (s, 18H, *t*Bu), 1.59 (s, 9H, *t*Bu). ESI-MS. Calcd for C$_{68}$H$_{59}$N$_7$O$_3$ZnRe ([M − CF$_3$SO$_3$]$^+$): 1272.3. Found: 1272.5. IR (cm^{-1}, CHCl$_3$): 2036 (s, $\tilde{\nu}_{C=O\ fac}$), 1932 (s, br, $\tilde{\nu}_{C=O\ fac}$).

Crystals of **2** suitable for X-ray diffraction were obtained by the slow diffusion of *n*-hexane into a DCM solution of the compound. Crystal data: C$_{69}$H$_{59}$F$_3$N$_7$O$_6$ReSZn, MW = 1422.86, triclinic, space group $P\bar{1}$, a = 8.7260(8) Å, b = 9.8370(9) Å, c = 40.956(3) Å, α = 84.227(10)°, β = 84.429(11)°, γ = 72.995(7)°, V = 3336.3(5) Å^3, Z = 2, D_c = 1.416 g/cm^3, μ = 4.750 mm^{-1}, F(000) = 1436, θ range = 2.11−26.76°. Final R1 = 0.0925, wR2 = 0.2276, and S = 1.194 for 838 parameters and 5036

dx.doi.org/10.1021/ic302663c | Inorg. Chem. 2013, 52, 3190−3197

Scheme 2. Synthesis of Dyad 4, with the Yield of Isolated Product in Each Step[a]

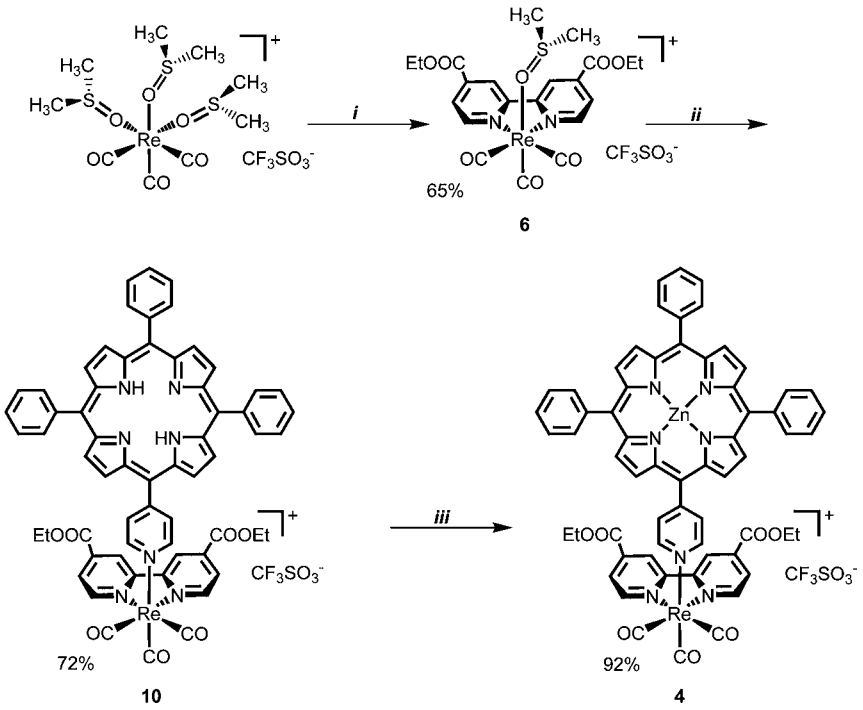

[a]Reagents and conditions: (i) 4,4′-DEC-bpy, acetone, reflux; (ii) 4′MPyP, $CHCl_3$, reflux; (iii) $Zn(OAc)_2·2H_2O$, $CHCl_3$/MeOH, room temperature.

unique reflections [R(int) = 0.0640], of which 3766 with $I > 2\sigma(I)$, max positive and negative peaks in ΔF map 1.538 (close to the disordered triflate) and −1.731 e/Å^3.

***fac*-[Re(CO)$_3$(bpy)(Zn·4′MPyd*t*BuP)](CF$_3$SO$_3$) (3).** Yield: 87%. ^{1}H NMR (δ, 500 MHz, CD_3OD): 9.54 (d, J = 5.7 Hz, 2H, H6,6′), 8.83 (m, 6H, βH), 8.77 (m, 4H, H2,6 + H3,3′), 8.60 (d, J = 4.7 Hz, 2H, βH), 8.45 (t, J = 8.2 Hz, 2H, H4,4′), 8.23 (d, J = 6.5 Hz, 2H, H3,5), 8.07 (d, J = 1.7 Hz, 2H, *o*H), 8.05 (d, J = 1.7 Hz, 4H, *o*H), 7.98 (t, J = 6.7 Hz, 2H, H5,5′), 7.89 (m, 3H, *p*H), 1.54 (s, 54H, *t*Bu). ESI-MS. Calcd for $C_{80}H_{83}N_7O_3ZnRe$ ([M − CF_3SO_3]$^+$): 1440.5. Found: 1440.5. IR (cm^{-1}, $CHCl_3$): 2036 (s, $\tilde{\nu}_{C=O\ fac}$), 1939 (s, br, $\tilde{\nu}_{C=O\ fac}$), 1926 (s, br, $\tilde{\nu}_{C=O\ fac}$).

***fac*-[Re(CO)$_3$(4,4′-DEC-bpy)(Zn·4′MPyP)](CF$_3$SO$_3$) (4).** Yield: 92%. ^{1}H NMR (δ, 400 MHz, $CDCl_3$): 9.49 (d, J = 5.7 Hz, 2H, H6,6′), 9.12 (s, 2H, H3,3′), 8.90 (m, 6H, βH), 8.69 (d, J = 5.1 Hz, 2H, βH), 8.59 (d, J = 6.4 Hz, 2H, H2,6), 8.38 (d, J = 5.5 Hz, 2H, H5,5′), 8.28 (d, J = 6.1 Hz, 2H, H3,5), 8.18 (d, J = 8.2 Hz, 2H, *o*H), 8.16 (d, J = 7.2 Hz, 4H, *o*H), 7.73 (m, 9H, *m*+*p*H), 4.52 (q, 4H, CH_2), 1.47 (t, 6H, CH_3). ESI-MS. Calcd for $C_{62}H_{43}N_7O_7ZnRe$ ([M − CF_3SO_3]$^+$): 1248.2. Found: 1248.4. IR (cm^{-1}, $CHCl_3$): 2038 (s, $\tilde{\nu}_{C=O\ fac}$), 1945 (s, br, $\tilde{\nu}_{C=O\ fac}$), 1935 (s, br, $\tilde{\nu}_{C=O\ fac}$), 1726 (m, $\tilde{\nu}_{C=O}$).

RESULTS AND DISCUSSION

The new dyads **2**−**4** were conveniently prepared via an efficient stepwise procedure from the cationic rhenium(I) precursor *fac*-[Re(CO)$_3$(DMSO-O)$_3$](CF$_3$SO$_3$); the bpy (or substituted bpy) ligand was introduced first, followed by the pyridylporphyrin. The last step was the insertion of zinc into the porphyrin core of the conjugate. As an example, the synthesis of dyad **4** is reported in Scheme 2.

Dyads **2**−**4** were characterized by ^{1}H NMR spectroscopy and ESI-MS. Figure 3 shows, as an example, the ^{1}H NMR spectrum of conjugate **4**; all the resonances were assigned by means of conventional H−H COSY experiments. It is worth noting that the resonance of the two pyridyl protons adjacent to the nitrogen atom (H2,6), which typically is shifted *downfield* upon binding to the {*fac*-Re(CO)$_3$}$^+$ fragment, in this case is shifted

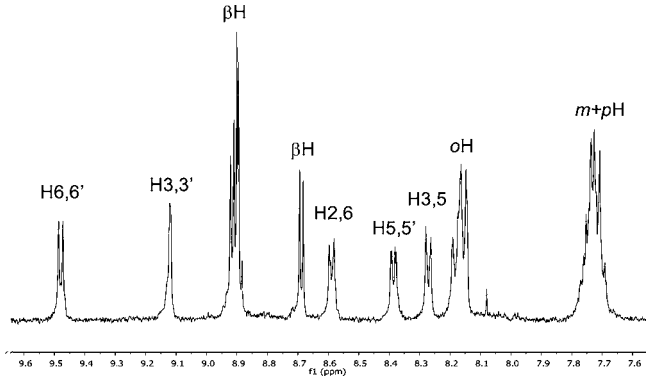

Figure 3. Downfield region of the ^{1}H NMR spectrum of conjugate **4** ($CDCl_3$, 400 MHz). See Figure 2 for the labeling scheme.

upfield compared to the unbound porphyrin because the protons fall into the shielding cone of the adjacent bpy ligand.[10]

The X-ray molecular structure of the cation of **2** is shown in Figure 4. The coordination bond lengths and angles are unexceptional and in agreement with those of similar rhenium(I) porphyrin conjugates previously described by us.[3]

As a model for the rhenium acceptor unit, we also prepared complex **7** by treatment of the common intermediate **6** with a slight excess of pyridine in a DCM solution at room temperature. Complex **7** was characterized in solution by ^{1}H NMR spectroscopy and in the solid state by X-ray crystallography (see the Supporting Information).

Electrochemical Behavior of Dyads 3 and 4. The electrochemical properties of dyads **3** and **4** were examined by cyclic voltammetry (CV) in a DCM solution [electrochemical window from +1.0 to −1.5 V, with saturated calomel electrode (SCE) as the reference electrode], focusing on the potential values for the first oxidation and reduction processes. For

dx.doi.org/10.1021/ic302663c | *Inorg. Chem.* 2013, 52, 3190−3197

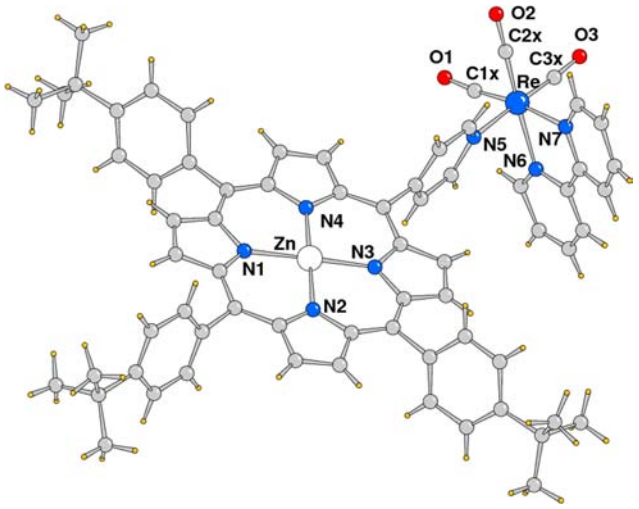

Figure 4. Molecular structure of the complex cation of **2** with a selected atom-labeling scheme. Coordination bond distances (Å): Zn–N1 2.031(12), Zn–N2 2.058(16), Zn–N3 2.020(13), Zn–N4 2.026(16), Re–C1x 1.741(18), Re–C2x 1.727(19), Re–C3x 1.715(15), Re–N5 2.094(16), Re–N6 2.19(2), Re–N7 2.09(2).

comparison, the zincated *meso*-tetraphenylporphyrins (Zn·TPP, Zn·*t*BuTPP, and Zn·d*t*BuTPP) and the rhenium model complexes *fac*-[Re(CO)$_3$(bpy)(py)](CF$_3$SO$_3$) and **7** were studied in the same experimental conditions. The results are summarized in Table 1. The data for dyad **1**, previously investigated by us,[3b] are also reported for comparative purposes. The results obtained for the reference porphyrins (Table 1) clearly show that the introduction of the electron-donor *t*Bu substituents on the *meso*-phenyl rings has only a small effect on the oxidation potential of the porphyrin. Conversely, the presence of the electron-withdrawing ethyl ester groups on the bpy ligand causes a large positive shift (ca. 0.4 V) in the reduction potential of the rhenium unit, which thus becomes significantly easier to reduce. In the cyclic voltammogram of dyad **4**, the first oxidation process is assigned to zinc porphyrin, whereas the first reduction process involves the bpy ligand of the rhenium unit (see the SI). As expected by a comparison with similar systems,[3,11] this voltammetric behavior is a good superposition of those of the molecular components, indicating the supramolecular nature of the conjugates investigated. Accordingly, the effects induced by functionalization on the model compounds are found to be almost identical also in the dyads: compare the oxidation potentials of **1** and **3** and the reduction potentials of **1** and **4**.

Photophysical Behavior of Dyads 2–4. A detailed photophysical investigation on the new dyads **2**–**4** was carried out in a DCM solution by stationary and time-resolved absorption and emission spectroscopy. For dyad **4**, some kinetic measurements were also performed in propionitrile and toluene for comparative purposes.

The absorption spectra of the three dyads are practically identical and dominated in the whole spectral region by the zinc porphyrin component, with two typical Q bands between 500 and 700 nm in addition to the Soret band at ca. 400 nm (see the SI). The rhenium unit does not absorb in the visible region, while in the UV region, it exhibits a metal-to-ligand charge-transfer Re → bipy band at ca. 350 nm, hidden by the porphyrin Soret band, and intense ligand-centered transitions below 330 nm (see the SI).

The results of the emission experiments are collected in Table 2. Following excitation in the visible region, dyads **2** and **3** showed typical porphyrin-based fluorescence. Comparative experiments carried out on optically matched solutions of **2** and **3g** and of the corresponding zinc porphyrin models at an excitation wavelength of 550 nm, clearly evidenced that the moderate fluorescence quenching observed for the rhenium dyads (both intensity and lifetime) is attributable, as previously discussed for **1**,[3] to the heavy-atom effect. These results are consistent with CV measurements (Table 1; compare **1** and **3**) showing that the introduction of the electron-donor *t*Bu substituents on the *meso*-phenyl rings has little effect on the

Table 2. Emission Properties of Dyads 1–4 and of the Model Compounds[a]

compound	λ_{max}(em), nm	Φ_0/Φ[b]	τ,[c] ns	τ_0/τ[b]
Zn·TPP	599, 645		1.7	
Zn·*t*BuTPP	601, 648		1.6	
Zn·d*t*BuTPP	597, 647		1.7	
1[d]	607, 650	1.6	0.9	2.0
2	613, 650	2.0	0.7	2.3
3	610, 650	1.9	0.6	2.8
4	596, 644	8.3	<0.25	>6.8

[a]Selective excitation of the zinc porphyrin component in the Q-band region (λ_{exc} = 550 nm), room temperature, and DCM solution. [b]Φ_0 and τ_0 are respectively the fluorescence quantum yield and lifetime of the corresponding zinc porphyrin model. [c]Estimated error: ±0.1 ns. [d]From ref 3.

Table 1. Electrochemical Data for Dyads 3 and 4 and for the Reference Compounds[a]

compound	$E_{1/2}$(red), V	$E_{1/2}$(ox), V	$E^{0-0}(S_1)$,[b] eV	ΔG,[c] eV
Zn·TPP	−1.38	+0.80		
Zn·*t*BuTPP	−1.50	+0.75		
Zn·d*t*BuTPP	−1.50	+0.74		
fac-[Re(CO)$_3$(bpy)(py)](CF$_3$SO$_3$)	−1.13			
fac-[Re(CO)$_3$(4,4′-DEC-bpy)(py)](CF$_3$SO$_3$) (**7**)	−0.72			
fac-[Re(CO)$_3$(bpy)(Zn·4′MPyP)](CF$_3$SO$_3$) (**1**)[d]	−1.16	+0.83	2.04	−0.05
fac-[Re(CO)$_3$(bpy)(Zn·4′MPyd*t*BuP)](CF$_3$SO$_3$) (**3**)	−1.15	+0.79	2.03	−0.09
fac-[Re(CO)$_3$(4,4′-DEC-bpy)(Zn·4′MPyP)](CF$_3$SO$_3$) (**4**)	−0.71	+0.88	2.02	−0.42

[a]All measurements were made in argon-purged DCM solutions at 298 K [0.1 M TBA(PF$_6$) as the supporting electrolyte, scan rate 200 mV/s, SCE as the reference electrode, and glassy carbon as the working electrode]. Half-wave potentials calculated as an average of the cathodic and anodic peaks (ΔE_p = 60–80 mV). [b]Estimated from the fluorescence spectrum. [c]Free-energy change for photoinduced electron transfer from the excited (S_1) zinc porphyrin unit to the rhenium unit.[17] [d]From ref 3b.

dx.doi.org/10.1021/ic302663c | Inorg. Chem. 2013, 52, 3190–3197

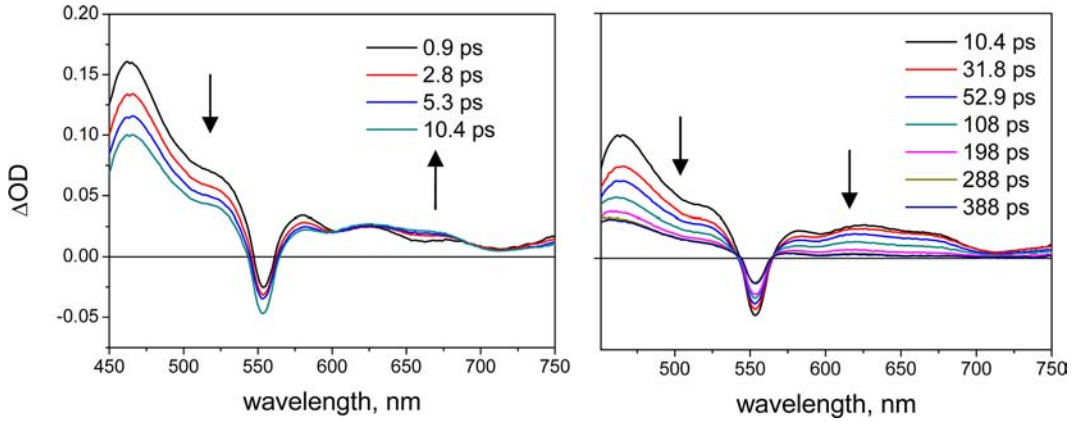

Figure 5. Transient spectral changes obtained for dyad **4** in a DCM solution (λ_{exc}= 560 nm) in the 0−10 ps range (left) and in the 10−400 ps range (right).

oxidation potential of the porphyrin. As a consequence, the driving force for the photoinduced electron-transfer process from the singlet excited state of zinc porphyrin to the rhenium unit improves negligibly on going from **1** to **3** (ΔG = −0.05 eV for **1** vs ΔG = −0.09 for **3**). Accordingly, also in dyads **2** and **3**, this process does not occur. By contrast, a strong quenching of the fluorescence intensity and lifetime (with respect to the reference Zn·TPP) was observed for dyad **4** (see the SI and Table 2).[12] The lifetime of the residual emission is shorter (<250 ps) than the instrumental response. These results clearly indicate that in dyad **4** there is an additional and efficient (100%) process for deactivation of the singlet excited state of zinc porphyrin that involves the rhenium(I) unit.

Ultrafast absorption measurements were performed to obtain information on the quenching mechanism. When excitation of **4** was carried out at 560 nm, where light is selectively absorbed by the zinc porphyrin, the spectral changes shown in Figure 5 were observed. The behavior is clearly biphasic, with different spectral changes taking place in the 0−10 and 10−400 ps time ranges (Figure 5). The initial spectrum of Figure 5, taken immediately after the excitation pulse (t = 0.9 ps), is typical for the zinc porphyrin singlet excited state:[13] a broad intense positive absorption in the 450−550 nm region and a relatively flat positive absorption throughout the 550−750 nm visible region with a superimposed bleaching of the ground-state Q bands at 565 (hidden within the excitation window) and 610 nm. Additional apparent bleaches at 625 and 670 nm are caused by stimulated emission. In the 1−10 ps time interval (Figure 5, left), the spectral changes show a substantial recovery of the bleach in the 520−680 nm range, accompanied by an increase in the optical density of the positive absorption in the 620−700 nm range, where at 660 nm the typical absorption band of the radical cation of zinc porphyrin can be easily recognized.[14] We attribute these spectral changes to the formation of the charge-separated product Zn^{+}−Re^{-} in which the zinc porphyrin chromophore is oxidized and the rhenium unit is reduced. In the longer time range (Figure 5, right), the spectroscopic signatures of the charge-separated state disappear with a uniform decay of the whole spectrum toward the initial baseline with isosbestic points at zero differential absorbance. This clearly indicates that Zn^{+}−Re^{-} converts quantitatively by charge recombination to the ground state.[15] Kinetic analysis of the spectral changes at 660 nm yields a time constant of 4 ps for charge separation and 96 ps for the charge-recombination process (Figure 6). These ultrafast experiments clearly show

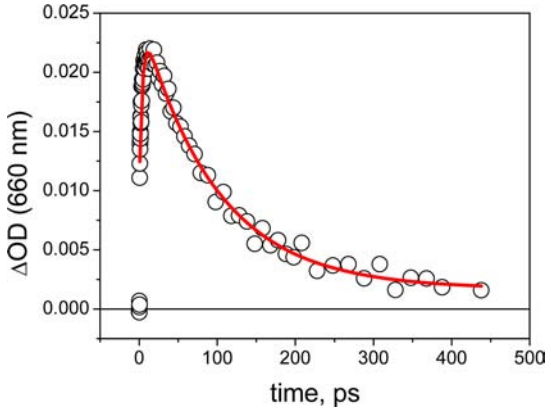

Figure 6. Kinetic analysis of the changes of the transient spectrum of **4** at 660 nm in DCM.

that in dyad **4**, in which 4,4′-DEC-bpy replaces bpy on the rhenium(I) acceptor fragment (compare **1** and **4**), an efficient and ultrafast intramolecular electron-transfer process occurs from the excited zinc porphyrin to the rhenium unit. These results can be explained on the basis of the energy level diagram (Figure 7) in which the charge-separated state Zn−Re^{-}, whose energy is calculated at 1.6 eV from the electrochemical results (Table 1), lies lower than the local singlet state (S_1) of zinc porphyrin [$E(S_1)$ = 2.02 eV, estimated from the fluorescence spectrum]. Thus, in dyad **4** the photoinduced electron-transfer process from excited zinc porphyrin to the rhenium unit has ΔG = −0.42 eV (i.e., ca. 0.4 eV more negative than that for **1**−**3**). Consistent with the fast rate measured by ultrafast spectroscopy (time constant = 4 ps), the charge-separation process falls in the normal Marcus region according to the standard electron-transfer theory.[16] Conversely, the rate for the charge-recombination process to the ground state is much slower (time constant = 96 ps) because it belongs to the Marcus inverted region (ΔG = −1.6 eV). Since the energy of the charge-separated state depends strongly on the solvent polarity, photophysical characterization of **4** was repeated in a solvent of higher polarity (propionitrile, PrCN) and in one of lower polarity (toluene) compared to DCM. Stationary emission measurements clearly indicated that in both solvents, as in DCM, fluorescence of zinc porphyrin was almost completely quenched. Ultrafast laser experiments in PrCN and toluene gave transient spectral changes qualitatively similar to those observed in DCM (see the SI), indicating that, in each

dx.doi.org/10.1021/ic302663c | Inorg. Chem. 2013, 52, 3190−3197

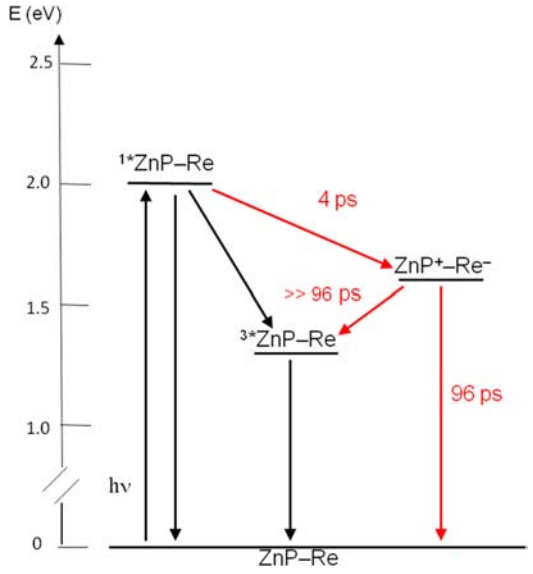

Figure 7. Energy level diagram for dyad **4** in a DCM solution.

case, a fast charge separation (i.e., formation of ZnP^+-Re^-), followed by slower recombination, occurred. However, the kinetics of the processes were found to be solvent-dependent. This is particularly true for the charge-recombination process, which slows down with decreasing solvent polarity. Kinetic analysis of the spectral changes (biexponential fitting performed at 660 nm; see the SI) gives the values of the time constants for the charge-separation and charge-recombination processes reported in Table 3.

Table 3. Time Constants (τ) for the Charge-Separation (CS) and Charge-Recombination (CR) Processes of Dyad 4 in Different Solvents (ε is the Dielectric Constant)

solvent	τ^{CS},[a] ps	τ^{CR},[a] ps	ε
PrCN	5	25	27.7
DCM	4	96	9.1
toluene	22	130	2.4

[a]Experimental error: ±10%.

The observed effect of the solvent on the electron-transfer rates can be qualitatively explained in terms of standard electron-transfer theory as a consequence of the changes in the driving force and reorganization energy.[16] In DCM, where $\Delta G = -0.42$ eV, the charge-separation process, assuming that the reorganization energy has a value of ca. 1 eV, falls in the normal Marcus region, whereas the charge recombination belongs to the Marcus inverted region. As the solvent polarity decreases, the energy of the charge-separated state rises; as a consequence, the driving force for charge recombination to the ground state grows, while the reorganization energy diminishes. In the Marcus inverted region, both factors act in the same direction, and thus a strong decrease in the rate with decreasing solvent polarity is predicted for the charge-recombination processes. On the other hand, for the charge-separation reactions that fall in the normal Marcus region, the two effects tend to compensate for each other, leading to prediction of much weaker solvent effects. The experimental results shown in Table 3 are consistent with these theoretical considerations: whereas the change from DCM to PrCN affects mainly the recombination time constant, the low polarity of toluene leads to a noticeable increase of the time constants for both processes. Overall, the observed electron-transfer kinetics is satisfactorily accounted for in terms of standard electron-transfer theory.

CONCLUSIONS

Ready-to-make and highly robust dyads of the type *fac*-$[Re(CO)_3(bpy)(Zn\text{·pyridylporphyrin})](CF_3SO_3)$, in which the zinc pyridylporphyrin chromophore behaves as photoactive and electron-donor moieties and the *fac*-$[Re(CO)_3(bpy)]^+$ unit as the electron acceptor, can be efficiently synthesized in a stepwise manner from the cationic rhenium(I) precursor *fac*-$[Re(CO)_3(DMSO\text{-}O)_3](CF_3SO_3)$. The modular procedure affords, with modest synthetic effort, tailor-made dyads whose properties can be tuned by changing, via appropriate functionalization, those of the bpy and porphyrin ligands.

As previously anticipated, we demonstrate here that a simple chemical modification of dyad **1**, i.e., functionalization of the bpy ligand with electron-withdrawing ethyl ester groups in the 4 and 4′ positions, greatly improves, as the rhenium unit becomes significantly easier to reduce, the thermodynamics of the photoinduced electron-transfer process ($\Delta G = -0.42$ eV vs $\Delta G = -0.05$ eV in **1**). As a consequence, whereas dyad **1** shows no evidence for the formation of the charge-separated state ZnP^+-Re^- (unless when in the presence of excess pyridine), in the new dyad **4**, an efficient and ultrafast intramolecular electron-transfer process occurs upon excitation with visible light. On the contrary, the introduction of electron-donor *t*Bu groups (either three or six) on the *meso*-phenyl moieties of zinc porphyrin has a negligible effect on the photophysics of the system.

Ultrafast time-resolved experiments performed at 560 nm on dyad **4** in DCM afforded a time constant of 4 ps for the charge-separation process and 96 ps for the subsequent charge-recombination process. Moreover, experiments performed in solvents of higher (propionitrile) or lower polarity (toluene) compared to DCM consistently suggest that the charge-separation process occurs in the normal Marcus region, whereas the charge recombination belongs to the Marcus inverted region. Clear evidence for the photoinduced electron-transfer quenching of a zinc porphyrin unit covalently connected to a Re(bpy) fragment was obtained by Perutz using time-resolved ultrafast IR spectroscopy.[11] As we already pointed out in a previous paper,[3] it is difficult to compare the kinetics of the electron-transfer processes for the dyad described by Perutz and **4** because, despite the similarity of the molecular photoactive components, the two systems are structurally different. However, in both cases, the lifetime of the charge-separated state might be too short (tens of picoseconds) to be useful for chemical reactions. Still, we are presently testing dyad **4** in the reaction of photoreduction of CO_2 (in the presence of an appropriate sacrificial electron donor). Our current work is also aimed at improving the photophysical properties of these dyads by further modifying the nature of the ligands, or by introducing additional redox-active components, in order to assemble triad systems with the final goal of increasing the lifetime of the charge-separated state.

ASSOCIATED CONTENT

Supporting Information

Additional spectroscopic and electrochemical characterization (ESI-MS, UV/vis, emission, CV, time-resolved experiments), decay analysis, and X-ray crystallographic data in CIF format for

dx.doi.org/10.1021/ic302663c | Inorg. Chem. 2013, 52, 3190−3197

7 and 2. This material is available free of charge via the Internet at http://pubs.acs.org.

AUTHOR INFORMATION

Corresponding Author

*E-mail: eiengo@units.it (E.I.), idm@unife.it (M.T.I.).

Present Address

‡T.G.: Center for Nano Science and Technology@PoliMi, Istituto Italiano di Tecnologia, Via G. Pascoli 70/3, 20133 Milano, Italy.

Notes

The authors declare no competing financial interest.

ACKNOWLEDGMENTS

Financial support from Prin2008 Grant 20085ZXFEE and Fondazione Beneficentia Stiftung is gratefully acknowledged. E.I. wants to acknowledge financial support from Reintegration Grant PERG02-GA-2007-224823. We thank Prof. E. Alessio and Prof. F. Scandola for helpful discussions.

REFERENCES

(1) (a) Barber, J. *Chem. Soc. Rev.* **2009**, *38*, 185−196. (b) Gust, D.; Moore, T. A.; Moore, A. L. *Acc. Chem. Res.* **2009**, *42*, 1890−1898. (c) Fontacave, A. F.; Artero, V.; Pereira, A.; Fontacave, M. *Dalton Trans.* **2008**, 5567−5569. (d) Li, X.; Wang, M.; Zhang, S.; Pan, J.; Na, Y.; Liu, J.; Åkermark, B.; Sun, L. *J. Phys. Chem. B* **2008**, *112*, 8198−8202. (e) Esswein, A. J.; Nocera, D. G. *Chem. Rev.* **2007**, *107*, 4022−4047.

(2) (a) Agarwal, J.; Fujita, E.; Schaefer, H. F.; Muckerman, J. T. *J. Am. Chem. Soc.* **2012**, *134*, 5180−5186. (b) Windle, C. D.; Câmpian, M. V.; Duhme-Klair, A.-K.; Gibson, E. A.; Perutz, R. N.; Schneider, J. *Chem. Commun.* **2012**, *48*, 8189−8191. (c) Yamamoto, Y.; Tamaki, Y.; Yui, T.; Koike, K.; Ishitani, O. *J. Am. Chem. Soc.* **2012**, *132*, 11743−11752. (d) Schneider, J.; Vuong, K. Q.; Calladine, J. A.; Sun, X.-Z.; Whitwood, A. C.; George, M. W.; Perutz, R. N. *Inorg. Chem.* **2011**, *50*, 11877−11889. (e) Kiyosawa, K.; Shiraishi, N.; Shimada, T.; Masui, D.; Tachibana, H.; Takagi, S.; Ishitani, O.; Tryk, D. A.; Inoue, H. *J. Phys. Chem. C* **2009**, *113*, 11667−11673. (f) Morris, A. J.; Meyer, G. J.; Fujita, E. *Acc. Chem. Res.* **2009**, *42*, 1983−1994.

(3) (a) Ghirotti, M.; Chiorboli, C.; Indelli, M. T.; Scandola, F.; Casanova, M.; Iengo, E.; Alessio, E. *Inorg. Chim. Acta* **2007**, *360*, 1121−1130. (b) Casanova, M.; Zangrando, E.; Iengo, E.; Alessio, E.; Indelli, M. T.; Scandola, F.; Orlandi, M. *Inorg. Chem.* **2008**, *47*, 10407−10418.

(4) Chiorboli, C.; Rodger, M. A. J.; Scandola, F. *J. Am. Chem. Soc.* **2003**, *125*, 483−491.

(5) Otwinowski, Z.; Minor, W. In Processing of X-ray Diffraction Data Collected in Oscillation Mode. *Methods in Enzymology, Macromolecular Crystallography*; Carter, C. W., Jr., Sweet, R. M., Eds.; Academic Press: New York, 1997; Vol. *276*, Part A, pp 307−326.

(6) Sheldrick, G. M. *Acta Crystallogr., Sect. A* **2008**, *A64*, 112−122.

(7) Farrugia, L. J. *J. Appl. Crystallogr.* **1999**, *32*, 837−838.

(8) (a) Fleischer, E. B.; Sacther, A. M. *Inorg. Chem.* **1991**, *30*, 3763−3769. (b) Alessio, E.; Macchi, M.; Heath, S. L.; Marzilli, L. G. *Inorg. Chem.* **1997**, *36*, 5614−5623.

(9) McCafferty, D. G.; Bishop, B. M.; Wall, C. G.; Hughes, S. G.; Mecklenberg, S. L.; Meyer, T. J.; Erickson, B. W. *Tetrahedron* **1995**, *51*, 1093−1106.

(10) Casanova, M.; Zangrando, E.; Munini, F.; Iengo, E.; Alessio, E. *Dalton Trans.* **2006**, 5033−5045.

(11) (a) Gabrielsson, A.; Hartl, F.; Zhang, H.; Lindsay Smith, J. R.; Towrie, M.; Vlcek, A., Jr.; Perutz, R. N. *J. Am. Chem. Soc.* **2006**, *128*, 4253−4266. (b) Gabrielsson, A.; Lindsay Smith, J. R.; Perutz, R. N. *Dalton Trans.* **2008**, 4259−4269.

(12) Quenching of the fluorescence of Zn·TPP (or Zn·*t*BuTPP or Zn·d*t*BuTPP) in the presence of complex 7, even at high concentrations (0.5 M), was not observed, thus confirming that a bimolecular electron-transfer process cannot occur because the lifetime of the zinc porphyrin singlet excited state is too short.

(13) Scandola, F.; Chiorboli, C.; Prodi, A.; Iengo, E.; Alessio, E. *Coord. Chem. Rev.* **2006**, *250*, 1471−1496.

(14) Fajer, J.; Borg, D. C.; Forman, A.; Dolphin, D.; Felton, R. H. *J. Am. Chem. Soc.* **1970**, *92*, 3451−3459.

(15) The ultrafast results demonstrate that in **4** the deactivation process from the charge-separated state $Zn^{+}-Re^{-}$, initially formed in a singlet spin state, toward formation of the ^{3}*ZnP−Re triplet does not favorably compete with the charge recombination to the ground state because it requires a spin inversion (see Figure 7).

(16) (a) Marcus, R. A.; Sutin, N. *Biochim. Biophys. Acta* **1985**, *811*, 265−322. (b) Newton, M. D. *Chem. Rev.* **1991**, *91*, 767−792.

(17) ΔG values were obtained as the difference between the energy of the singlet excited state of the porphyrin unit $[E^{0-0}(S_1)]$ and the energy of the charge-separated state $ZnP^{+}-Re^{-}$ inferred from electrochemical data (see Figure 7). No correction for the electrostatic work term is required in this case because of the charge shift character of the process involved.